



**Eberswalde University
for Sustainable
Development**



MIYA e.V.

Fachverband zur
Förderung der
Miyawaki-Methode

Integration of New Technologies in Tiny Forests: Personal Laser Scanner Case Study

Submitted by

Stefan Scharfe
Ramazan Bülbül

Supervisor

Prof Dr. Jan-Peter Mund

Eberswalde, May 2022

Table of content

1. INTRODUCTION	4
2. MATERIALS and METHODS	5
2.1. Study Area	5
2.2. Equipment for scanning	6
2.3. Workflow	8
2.4. Data Acquisition	9
2.5. Converting to Point Cloud Data	10
2.6. Data Processing	10
2.6.1. Clipping to the Area of Interest (AOI)	10
2.6.2. SOR Filter and Cloth Simulation Filter	11
2.6.3. Ground Points Interpolation	11
2.6.4. Poisson Surface Reconstruction	11
2.6.5. Volume Calculation 2.5	12
2.6.6. Point Cloud Thinning	12
2.6.7. Ground Classification	12
2.6.8. Digital Terrain Model	13
2.6.9. Terrain Normalization	13
2.6.10. Watershed Segmentation	13
2.7. Evaluation	14
3. RESULT AND DISCUSSION	15
3.1 Ground Points Interpolation	15
3.2 Poisson Surface Reconstruction	15
3.3 Volume Calculation 2.5	17
3.4 Digital terrain Model	17
3.5 Point Cloud Normalization and Canopy Height Model	18
3.6 Detection and localization of tree crowns	20
3.7 Tree Size Distribution	21
4. CONCLUSION	23
Bibliography	24

Table of figures

1: Location of the Tiny Forest in Zichow, Brandenburg, Germany.....	5
2: Technical specification of GeoSLAM Zeb Horizon	6
3: GeoSLAM ZEB Horizon on the mission in the Tiny Forest-Zichow	7
4:Workflow diagram for Tiny Forest	8
5: Representative Scan Route (top view of Plot I in Cloud Compare).....	9
6: a) Point cloud before clipping at 75 m scale in Cloud Compare b) Point Cloud after clipping to 17 m x 43.5 m.....	10
7: 2D illustration of the Poisson reconstruction.....	11
8: An illustration of watershed segmentation Algorithm. (a) A CMM, (b) the complement of the CMM, and (c) dams built at the divide line (Chen, 2006).	14
9: Interpolated Ground Points of Tiny Forest in CloudCompare.....	15
10: a) Poisson Surface Reconstruction of ‘interpolated ground points’	16
11: b) Poisson Surface Reconstruction of the merging of ‘interpolated ground points’ and ‘off-ground points’.....	16
12: Volume Calculation 2.5. Image is top view with “Ground” and “Ceil”	17
13: Creating Digital Terrain Model of Tiny Forest using inverse distance weighting (IDW) interpolation with 1 cm resolution in RStudio, front view.....	18
14: Normalized point cloud of Tiny Forest, front isometric view.....	19
15: Canopy Height Model of Tiny Forest, front isometric view.	19
16: Location of the tree crowns in Tiny Forest, top view in QGIS software.....	20
17: Crown Diameters Distribution.....	21
18: DHB Distribution.....	22
19: Height Distribution	22

1. INTRODUCTION

The consequences of climate change have long since arrived in Germany and, despite the successful reduction of CO₂ emissions and increasing environmental awareness among the population, the climate resilience of cities must be strengthened in order to meet the challenges of the future. In this respect, the concept of the Tiny Forest according to Akira Miyawaki offers a promising, holistic approach.

The Miyawaki method refers to an innovative planting methodology originating in Japan. It involves the establishment of site-appropriate, highly diverse forest ecosystems on small areas of 100 m² or more, which can be used primarily in urban areas, e.g. for climate adaptation, air filtration or to increase biodiversity. Areas of low ecological value are particularly suitable for this method, which can be transformed into self-sufficient ecosystems within a short period of time through appropriate soil regeneration and dense planting.

The non-profit association MIYA e.V., located in Eberswalde, plants Tiny Forests all around Germany since 2020. In collaboration with IT4Forest we tested the SLAM technology on one of the first Tiny Forest sites in Germany, in which a total of 2400 saplings were planted on 800 m² area.

Light Detection and Ranging (LIDAR) technology has made it possible to detect the vertical and horizontal distribution of a forest area. Apart from general application such as identifying the height, canopy and crown volume, and biomass calculation of a forest, it also allows more detail application such as individual tree delineation with 3D mapping (Duncanson, Cook, Hurtt, & Dubayah, 2014).

According to the used platforms, LIDAR technologies can be divided in four different classes: i. Spaceborne Laser Systems (SLS), ii. Airborne Laser System (ALS), iii. Terrestrial Laser System (TLS), and iv. Mobile Laser System (MLS). The most recent development is SLS, e.g., the GEDI systems, which mounted at the ISS and operates on a scope of global earth observation (Dubayah, 2020). ALS is based on LIDAR acquisition from an aircraft which gives georeferenced data for hundreds of ha. TLS are mounted on a stationary tripod scanning the direct surrounding. MLS, are also comparably new applications, requires a carrier that can be a vehicle (vehicle laser scanner (VLS)) or handled by a person (personal laser scanner (PLS)) (Xu, Sun, Yun, & Wang, 2020).

Personal Laser Scanner (PLS) makes the point cloud acquisition viable and efficient with the help of the inertial measurement units (IMU) and provides point cloud accuracy at a centimeter level (di Filippo, et al., 2018). Further, it simplifies the preparation processes and decreases the processing time compared to stationary terrestrial laser scanner (Cabo C, 2018). Especially, the development of the simultaneous localization and mapping (SLAM) technology and the robotic operative system (ROS) allows to on-the-fly

registration of point clouds and trajectories and the processing of 3D map without external positioning systems (Cabo C, 2018). Especially, point cloud data acquired by ALS provides information on a large area but with limited resolution, compared to PLS (Gollob, Ritter, & Nothdurft, 2020).

In this study, the point cloud data set captured by PLS where SLAM technology was used was tested as a part of integration series of new technologies in Tiny Forest.

2. MATERIALS and METHODS

2.1. Study Area

The study area is located in Zichow, which is a small village in the north-west of Brandenburg, Germany. In 2020 the first Tiny Forest of Germany was planted there on an area of 700 m² on private property (s. fig. 1).



1: Location of the Tiny Forest in Zichow, Brandenburg, Germany

2.2. Equipment for scanning

For the acquisition of the point cloud data, the personal laser scanner (PLS) was GeoSLAM Zeb Horizon was used. This scanner provides flexibility in outdoor scans with a range of 100-meter, lightweight, and user-friendly design (Solutions: ZEB Horizon, 2021). Further specifications can be found in figure 2.

Technical specification	
Range	100m
FOV	360° x 270°
Protection class	IP 54
Processing	Post
Data logger carrier	Backpack or shoulder strap
Scanner head weight	1.5kg
Datalogger weight (incl. battery)	1.3kg
Colourised point cloud	✓*
Intensity	✓
Referenced imagery	✓*
Scanner points per second	300,000
No. of sensors	16
Relative accuracy	1 - 3 cm**
Raw data file size	100-200MB /min

2: Technical specification of GeoSLAM Zeb Horizon

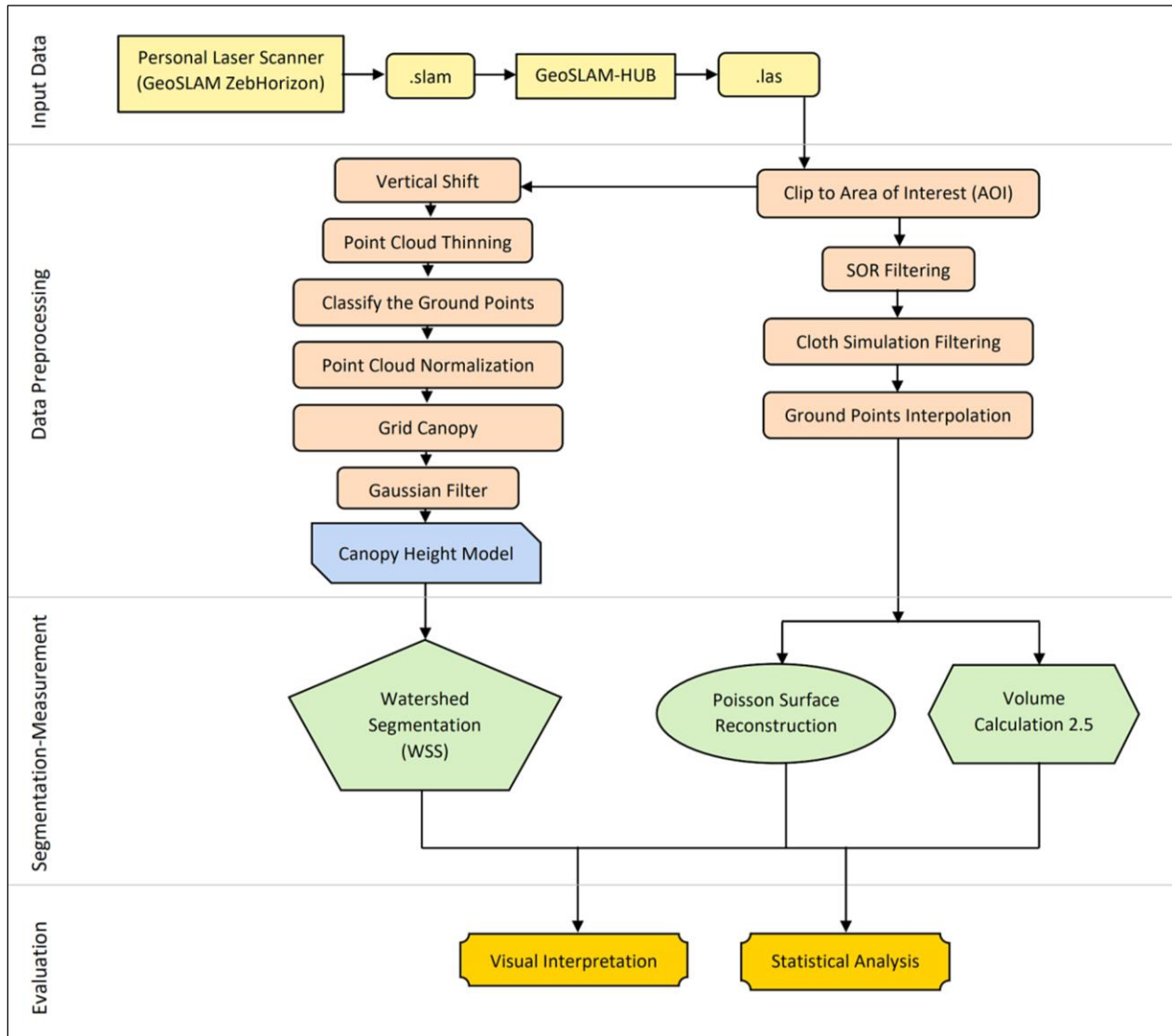


3: GeoSLAM ZEB Horizon on the mission in the Tiny Forest-Zichow

GeoSLAM ZEB Horizon scanner doesn't provide a global navigation satellite system (GNSS), but it contains an inertial measurement system (IMS) as a navigation unit. For this reason, it needs to define a local coordinate reference system with the vertical axis for each scan. To get reliable results, it needs to be activated in a horizontal position on a flat surface and must go back to starting point and position after each scan to close its circle (Nocerino, Menna, Remondino, Toschi, & Rodríguez-González, 2017).

2.3. Workflow

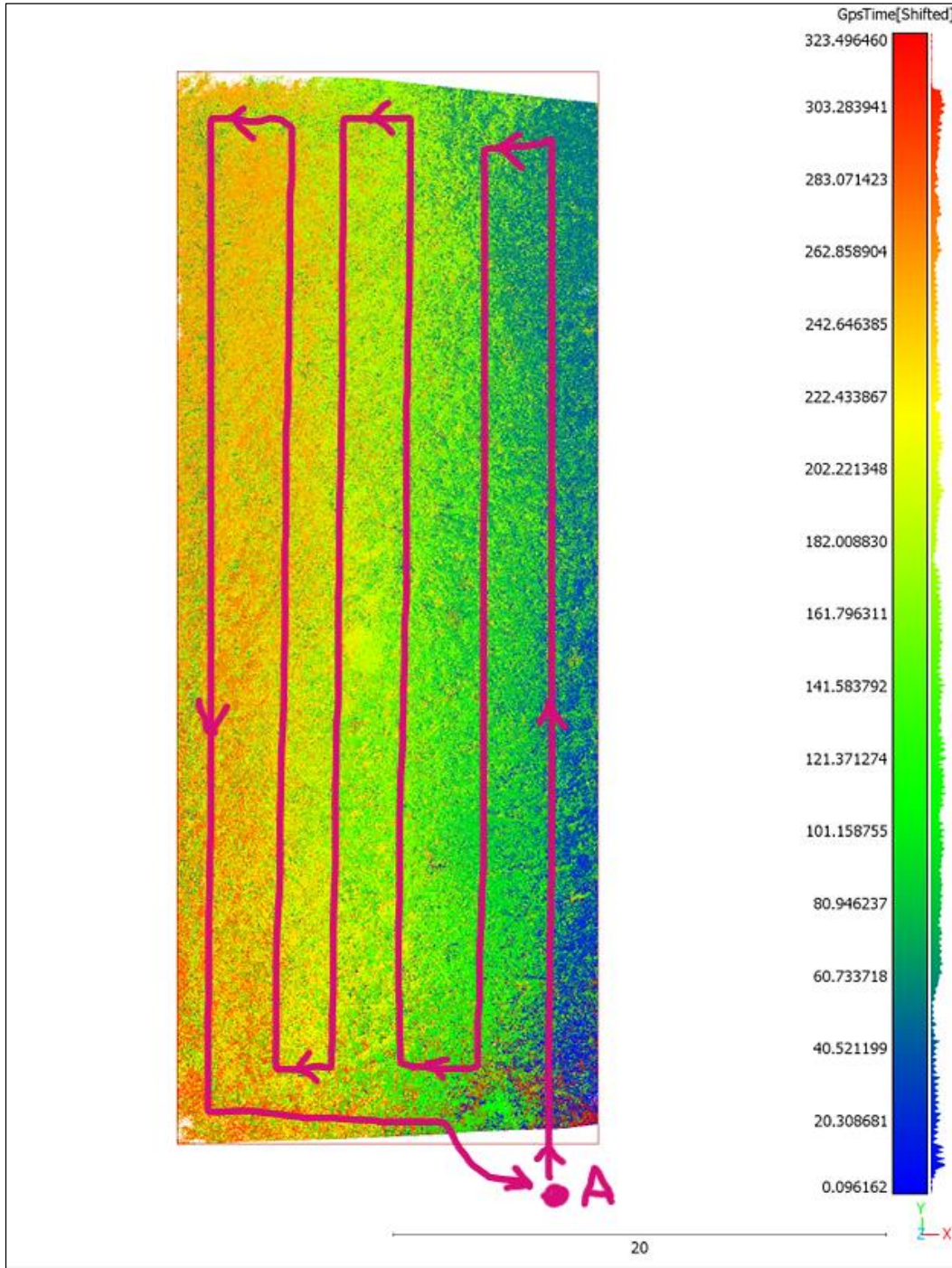
The illustrated workflow in the following Figure is described consecutive in the following chapters.



4:Workflow diagram for Tiny Forest

2.4. Data Acquisition

Tiny Forest field of 20m x 45m were scanned following a snake-wise pattern. The route starts at point "A" and finished in a closed path at the starting point (fig. 5).



5: Representative Scan Route (top view of Plot I in Cloud Compare)

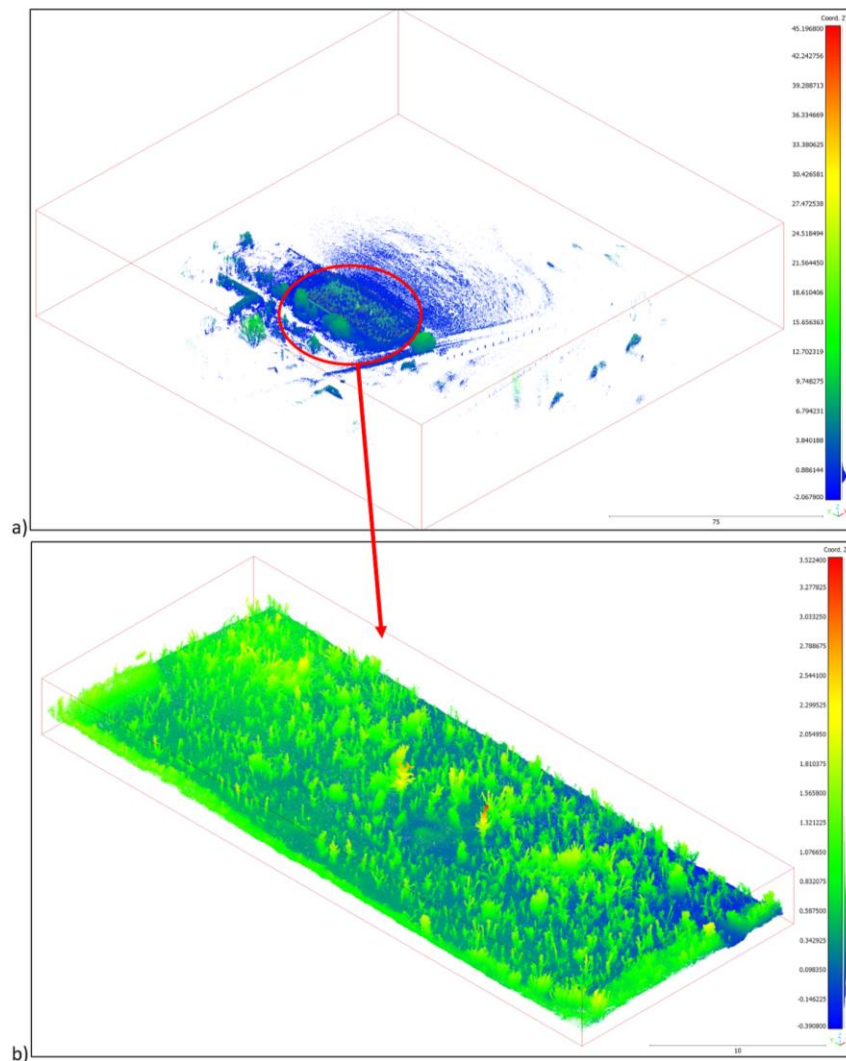
2.5. Converting to Point Cloud Data

Discrete Laser point data from the PLS scanner was processed to a point cloud using the GeoSLAM HUB. 'slam' data set converted into '.las' data set to make the data integration possible with various software such as CloudCompare, RStudio, QGIS etc.

2.6. Data Processing

2.6.1. Clipping to the Area of Interest (AOI)

These point clouds containing hundreds of meters of landscape due to the beam scatter capacity of the GeoSLAM Scanner, were clipped to the plot size of 20 m by 45 m, as can be seen in figure 6.



6: a) Point cloud before clipping at 75 m scale in Cloud Compare b) Point Cloud after clipping to 17 m x 43.5 m

2.6.2. SOR Filter and Cloth Simulation Filter

S.O.R. (Statistical Outlier Removal) filtering applied to the point cloud dataset, the mean distance to neighbors was taken as 6 neighbors and 1 standard deviation multiplier. The same values of the variables were applied at each step where SOR filtering was required in the whole process.

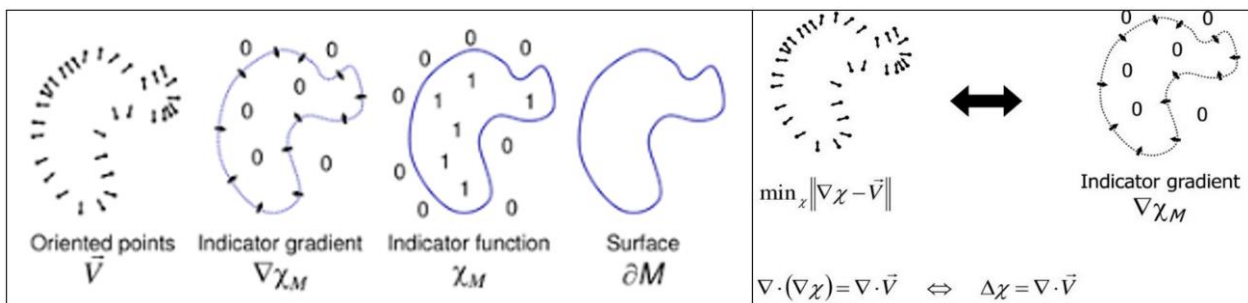
Formula: (the max distance will be: average distance + n * standard deviation)

For the further processes, ground points and off-ground point needed to be separated, the Cloth Simulation Filtering (CSF) was applied to the dataset. To do so, the point cloud is mirrored at a horizontal surface. Afterwards, a “soft cloth” is put above the upside-down point cloud. The final shape of the cloth is generated according to the distance between neighboring points depending on a threshold defined by the user or by default. Then, it is possible to classify the ground and the off-ground points (Zhang, et al., 2016).

2.6.3. Ground Points Interpolation

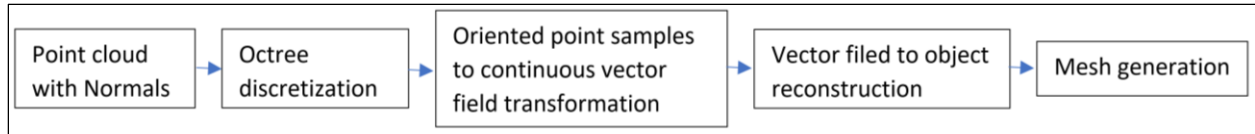
Ground points empty spaces mainly caused by the junction points of the tree stems were filled by ground interpolation at the 1 cm level.

2.6.4. Poisson Surface Reconstruction



7: 2D illustration of the Poisson reconstruction

The Poisson reconstruction provides a global solution for all data, uniformly or non-uniformly sampled points, by treating them at once, without dividing them into sections or blending them together. So, the Poisson reconstruction, creates very smooth surfaces that solidly approximate noisy data (Michael Kazhdan, 2006). Workflow of the Poisson Surface Reconstruction (Guarda, Andre F. R., 2017) described:



Normals of each dataset were computed with a 'quadric' surface approximation, good for curvy surfaces, within a 1cm radius neighbors and +Z axis orientation. Poisson Surface Reconstruction was applied to the each dataset with "Dirichlet" border structure, resulting in more accurate model (Michael Kazhdan, 2020), 12 level octree dept were choosen.

2.6.5. Volume Calculation 2.5

It is a grid-based volume calculation (Martin Štroner, 2019) that works by projecting one or two clouds in a 2D grid. Each time 'Ground/Before', 'Ceil/After', 'grid size', 'cell height', and 'empty cells integration' variables should be defined. In this study, the average cell height was taken for each 2D grid of 1 mm grid size and the empty cells were interpolated.

The calculation of volume relies on the following: (dV = grid step * grid step * difference of height)

2.6.6. Point Cloud Thinning

A lower point density does not considerably affect the accuracy of the results (Gargoum & El-Basyouny, 2019) while it reduces the processing time significantly (Pirotti & Tarolli, 2010). Further, it reduces the number of points along the allocation pathways and homogenizes the point density (Hämmerle & Höfle, 2014). The point clouds were thinned to 5000 points per square meter.

2.6.7. Ground Classification

For the classification of the ground points, the Progressive Morphological Filter (PMF) was applied. PMF gradually increases the window size and the elevation threshold to eliminate off-ground points and enables to acquire a terrain model of the remaining ground points (Zhang, et al., 2003)

Formula of 'window size' w_k

$$w_k = 2 \times k \times b + 1$$

where $k = 1, 2, \dots, M$ and b is initial and/or base window.
 Or $w_k = 2 \times b^k + 1$ (this formula is to decrease the number of iterations)

Formula of `elevation threshold`

$$s = \frac{dh_{\max(t),k}}{\frac{(w_k - w_{k-1})}{2}}$$

where `the maximum elevation difference` is $dh_{\max(t),k}$, s is the terrain slope (Zhang, et al., 2003).

2.6.8. Digital Terrain Model

A Digital Terrain Model (DTM) was generated from the previously classified ground points by using the Inverse Distance Weighting (IDW) interpolation algorithm. The closer(neighbor) reference points have more effect(weighting) on the IDW interpolation.

The formula of IDW interpolation fellows

$$z = \frac{\sum_{i=1}^n \frac{z_i}{d_i^p}}{\sum_{i=1}^n \frac{1}{d_i^p}}$$

where p is the speed reducer weight control rate according to distance, where it is equal 2, d_i is the distance from unknown point to a well-known point and z_i is the heigh of the point i (de Mesnard, 2013).

2.6.9. Terrain Normalization

The point could was normalized by subtracting the elevation of the corresponding DTM from each point, also called `Topographic Normalization`. (Liu, Skidmore, Heurich, & Wang, 2017):

$$H_{local} = H_{raw} - E_{ground}$$

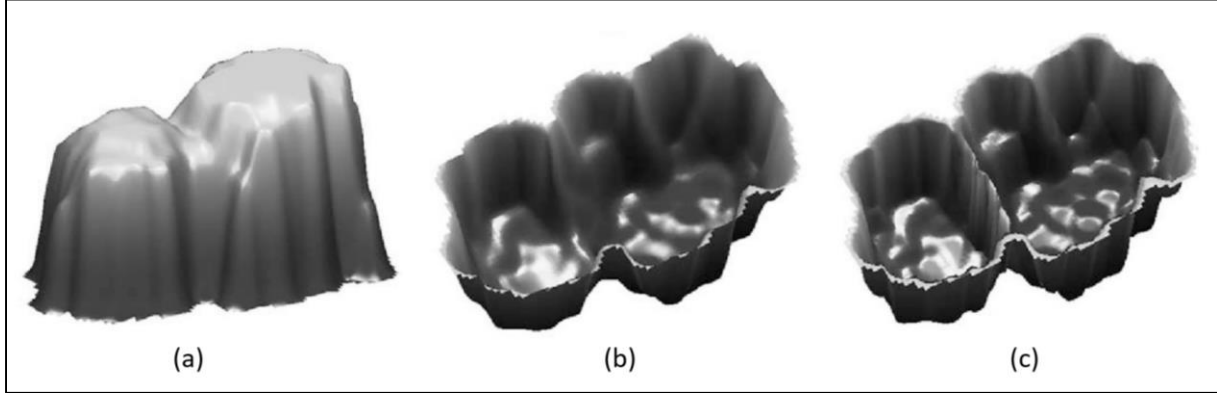
H_{raw} is the heigh of the vegetation point, E_{ground} is the elevation heigh of the ground, H_{local} is the normalized local heigh of the vegetation point (Liu, Skidmore, Heurich, & Wang, 2017).

The z-values of the resulting point cloud represent the elevation above the ground level of each point and enables to calculate a canopy height model (CHM) and further to derive individual tree heights and retrieve stand parameter like mean tree heigh or mean canopy height (Maguya, Junttila, & Kauranne, 2013).

2.6.10. Watershed Segmentation

Watershed Segmentation algorithm was applied to acquire the inventory of the Tiny Forest. First, the complement of the canopy maxima model (CMM) is generated. This model is presumed to be immersed in the water basin. Dividing lines are established to prevent the water from going to both trees and to

make the distinction for separating two neighboring trees and used to identify each individual tree (Chen, 2006).



8: An illustration of watershed segmentation Algorithm. (a) A CMM, (b) the complement of the CMM, and (c) dams built at the divide line (Chen, 2006).

In this segmentation, minima imposition filter is applied to complement of the CMM before detecting the watersheds to remove all non-treetop minima. f is the complement of the CMM, t_{max} is the maximum value f , and f_m is a marker image which is specified at each pixel p :

$$f_m(p) = \begin{cases} 0, & \text{if } p \text{ belong to a marker,} \\ t_{max} + 1, & \text{otherwise.} \end{cases}$$

First, minima imposition filter calculates a pixel-wise minimum between $f + 1$ and f_m , donated as $(f + 1)^{f_m}$, and then reconstruct by erosion of $(f + 1)^{f_m}$ from f_m :

$$f_{mp} = R_{(f+1)^{f_m}}^{\varepsilon}(f_m),$$

where f_{mp} is the image after minima imposition, $R_{(f+1)^{f_m}}^{\varepsilon}(f_m)$ is defined as the geodesic erosion of $(f + 1)^{f_m}$ with respect to f_m iterated until stability is reached (Soille, 2004). The geodesic erosion of $(f + 1)^{f_m}$ with respect to f_m is to perform morphological erosion for f_m , but the value of $(f + 1)^{f_m}$ is used only if the value of erosion is smaller than $(f + 1)^{f_m}$. Minima imposition can reconstruct the complement of CMM so that there are only minima corresponding to marked treetops (Chen, 2006).

2.7. Evaluation

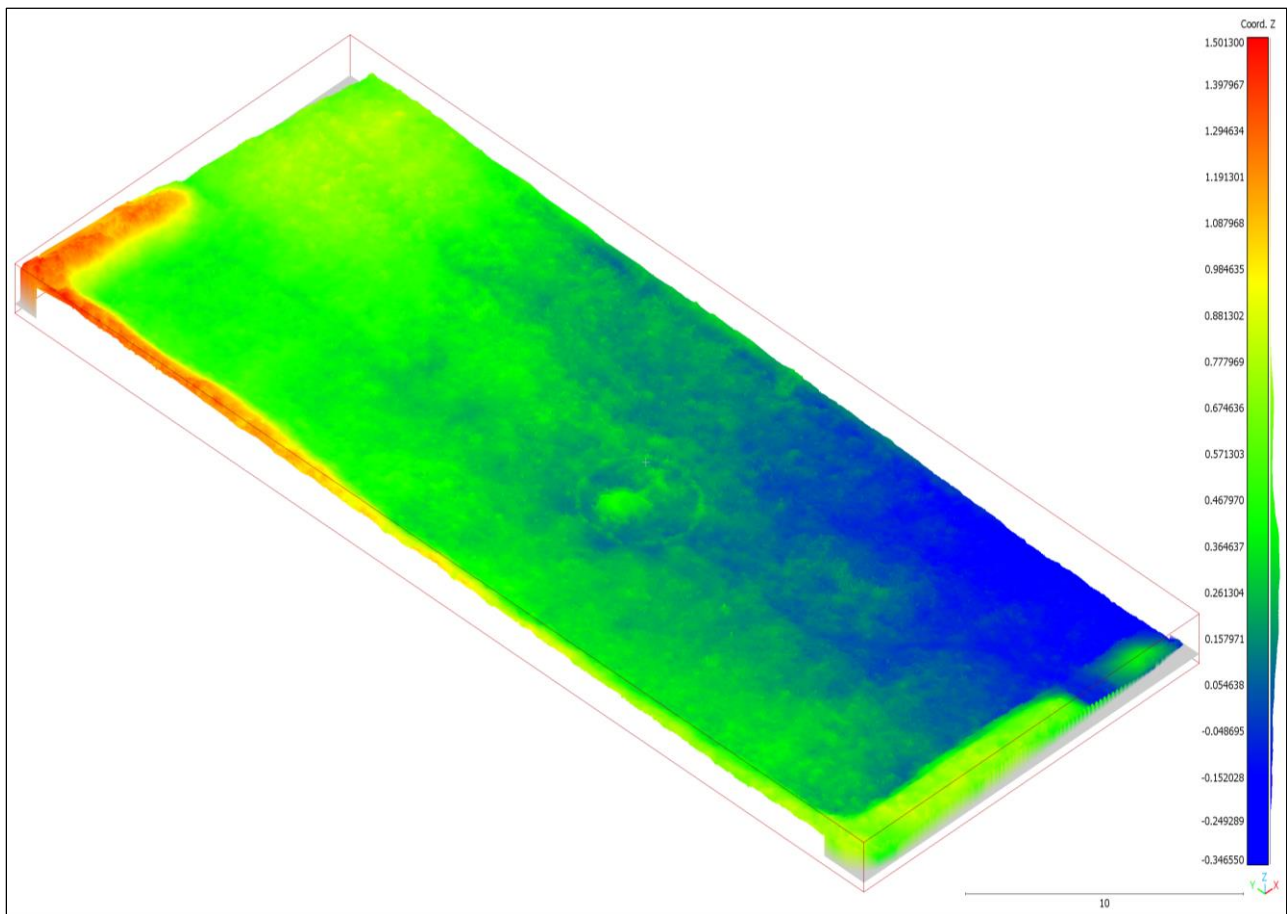
Evaluation of the various application int the Tiny Forest is presented at the Result and Discussion part of this study.

3. RESULT AND DISCUSSION

A point cloud-based (Poisson Surface Reconstruction) and a raster-based (Volume Calculation 2.5) approach were applied to the dataset to measure the amount of Wood contained in the Tiny Forest after 'Ground Points Interpolation'. In addition to these, especially the point cloud-based approach provides a clear visualization as it gives 3D results.

3.1 Ground Points Interpolation

Interpolated ground was to be based for the Poisson Surface Reconstruction and Volume Calculation 2.5, afterwards.



9: Interpolated Ground Points of Tiny Forest in CloudCompare

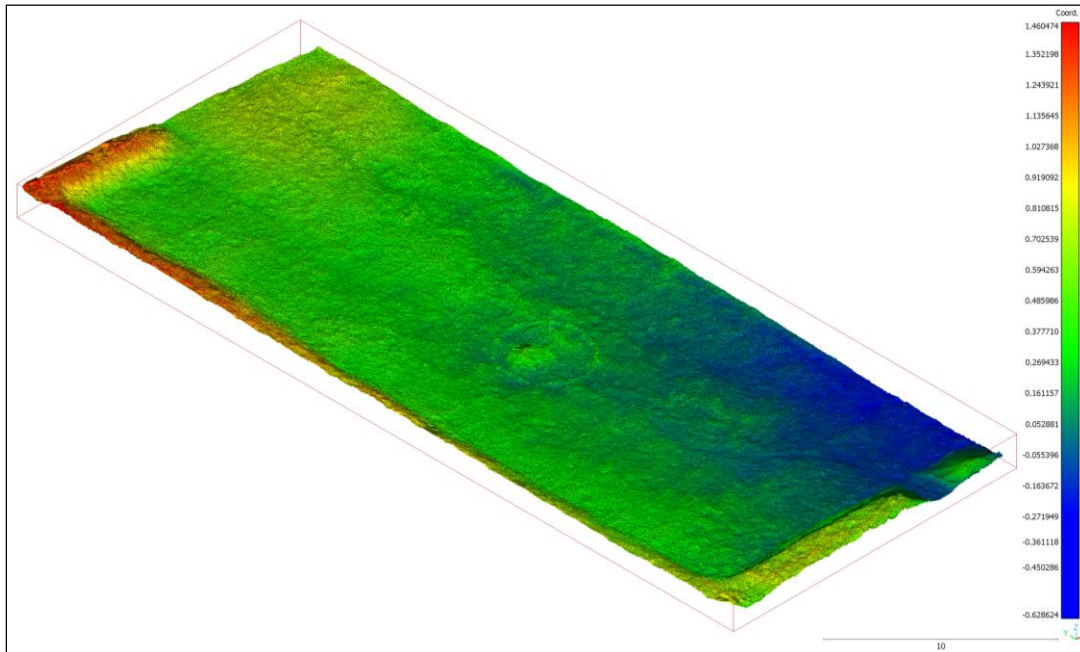
3.2 Poisson Surface Reconstruction

Surface of the interpolated ground and interpolated ground merged to off-ground points were reconstructed, and volume of each mesh has been executed.

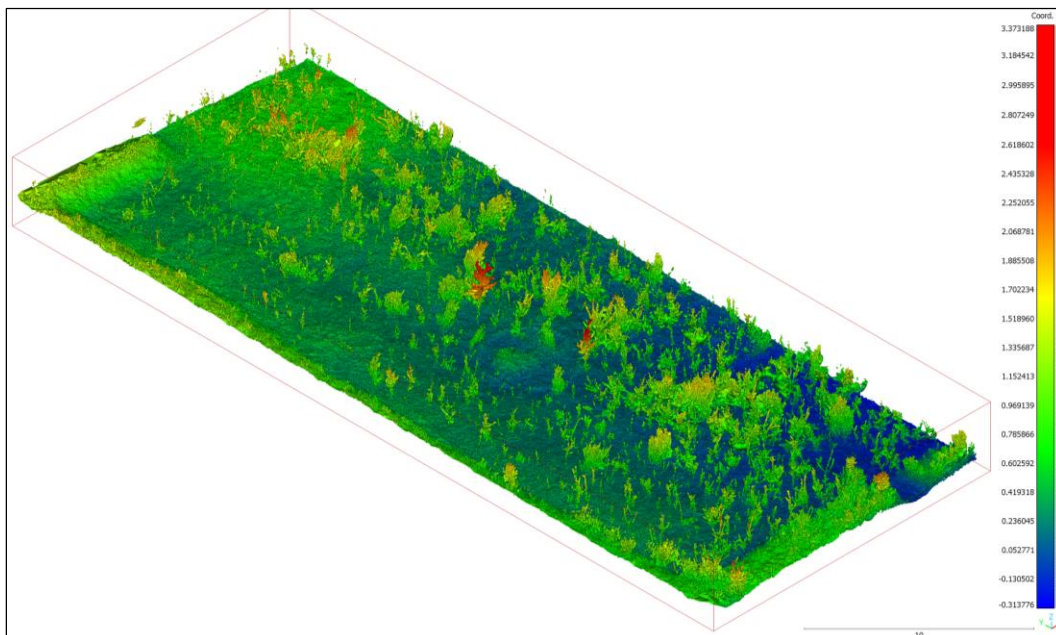
Finally, to find the amount of net wood in the Tiny Forest, the mesh volume calculation of the interpolated ground ($V=72.6454$ cubic meters) was subtracted from the mesh volume calculation of the merged dataset ($V=94.7012$ cubic meters).

According to Poisson Surface Reconstruction, the net amount of the wood in the Tiny Forest:

The amount of the wood in Tiny Forest = (Poisson recon (b)) - (Poisson recon (a)) = **22.1 cubic meters**



10: a) Poisson Surface Reconstruction of 'interpolated ground points'

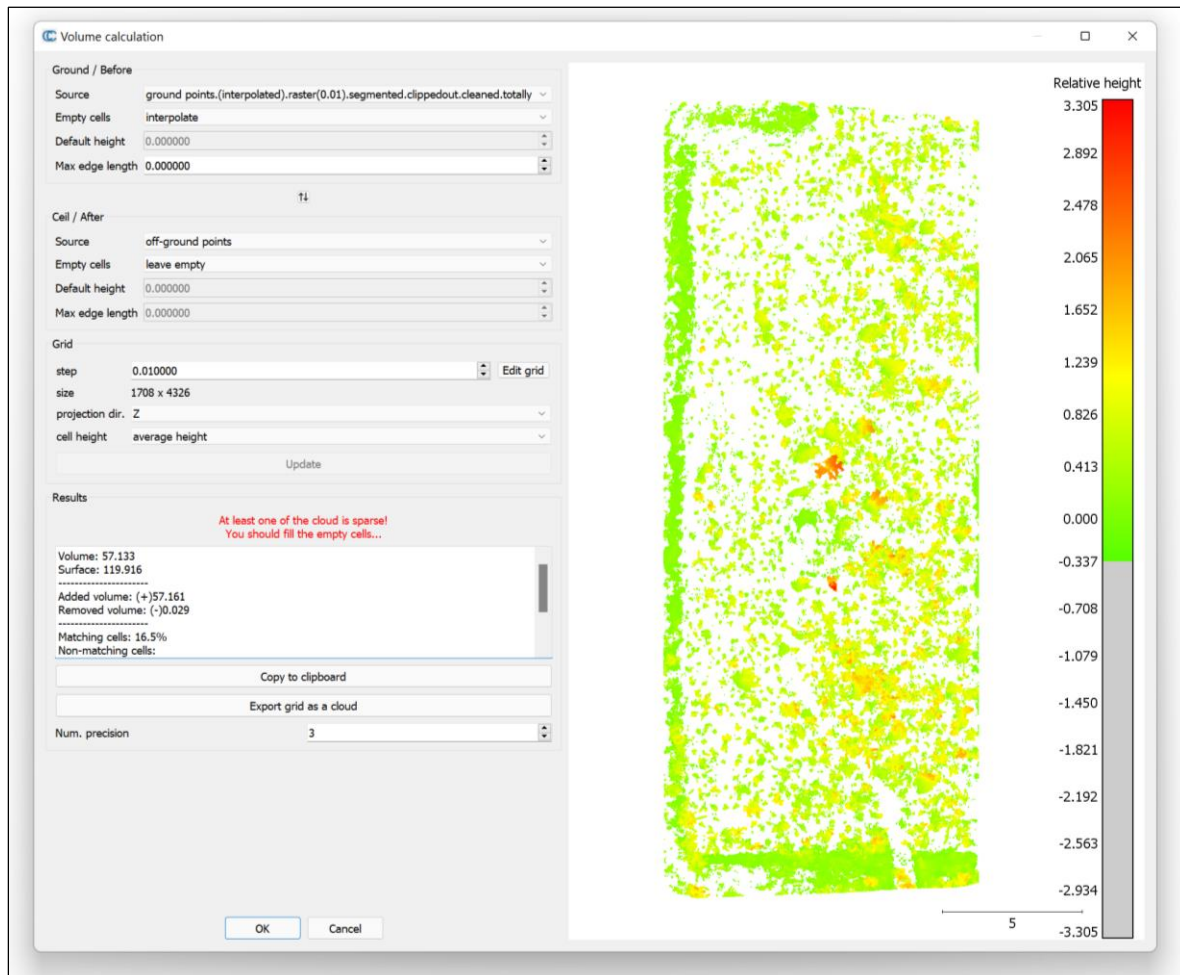


11: b) Poisson Surface Reconstruction of the merging of 'interpolated ground points' and 'off-ground points'

3.3 Volume Calculation 2.5

For approach Volume Calculation 2.5, which is raster-based, the 'interpolated ground' was chosen as "Ground" and 'off-ground' points as "Ceil", respectively. In this process, empty cells were filled by interpolating and grid steps were determined to be 1cm, see in the following Figure.

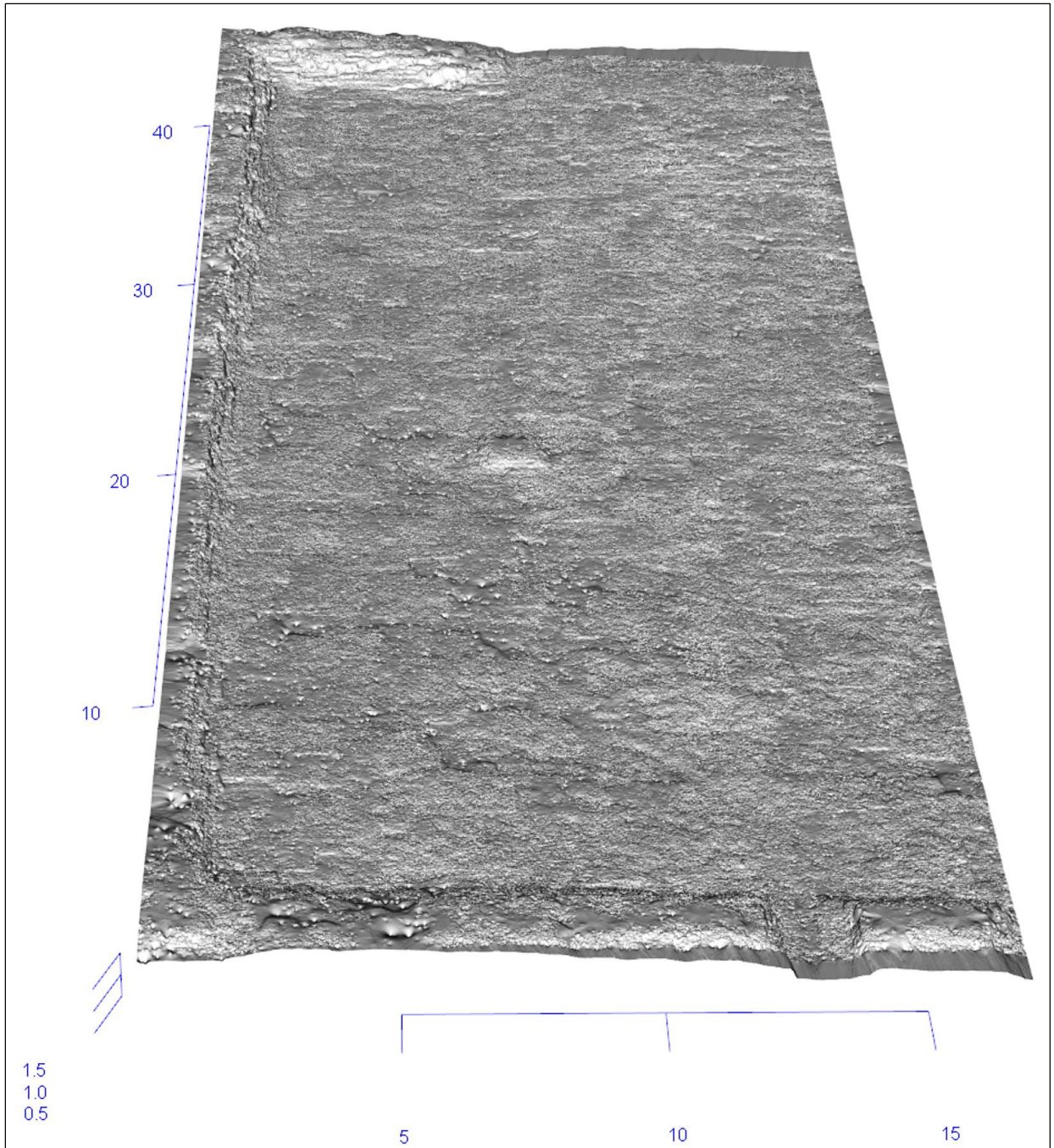
According to Volume Calculation 2.5 , the amount of the wood in Tiny Forest: **57.133 cubic meters**.



12: Volume Calculation 2.5. Image is top view with "Ground" and "Ceil"

3.4 Digital terrain Model

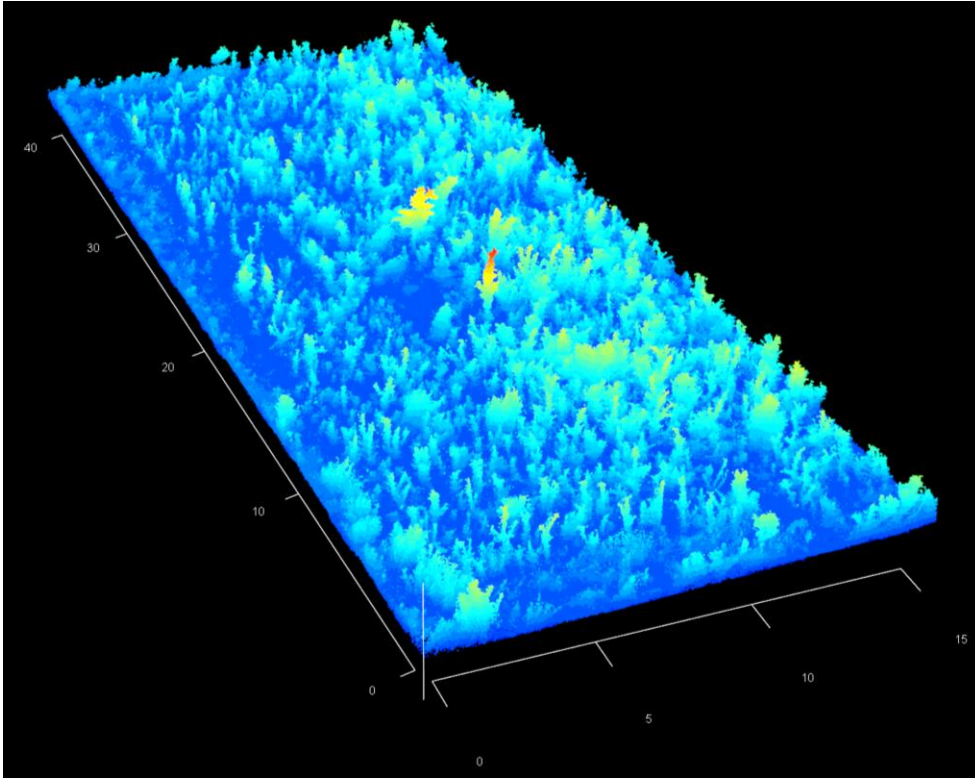
To examine the surface of Tiny Forest field, first, ground points were separated. Then, inverse distance weighting (IDW) interpolation was applied at 1 cm resolution in RStudio.



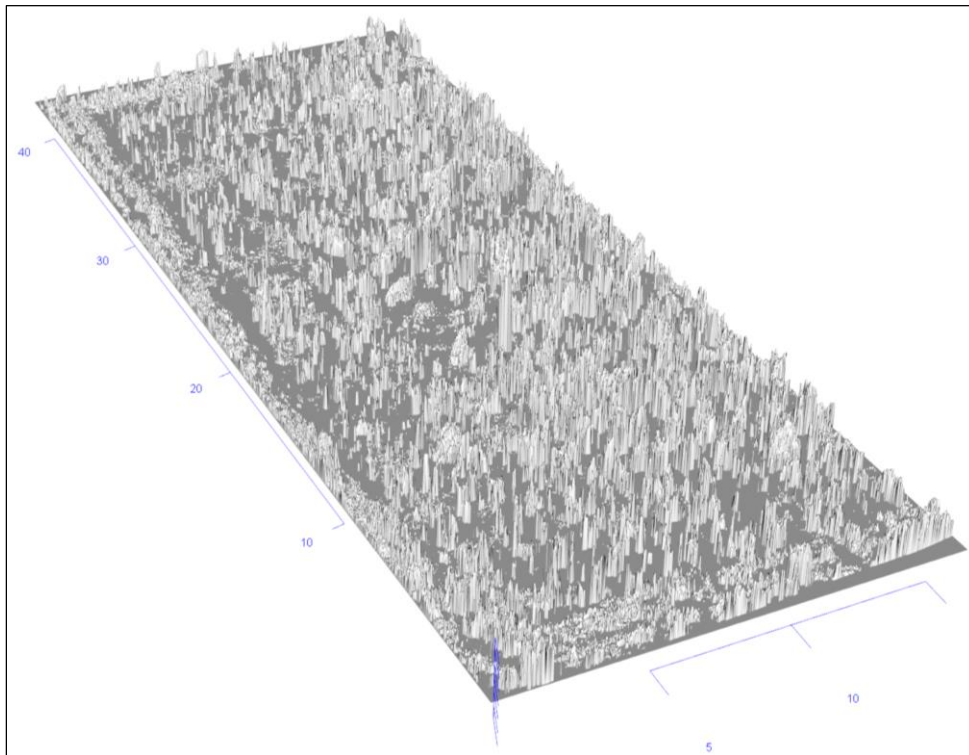
13: Creating Digital Terrain Model of Tiny Forest using inverse distance weighting (IDW) interpolation with 1 cm resolution in RStudio, front view.

3.5 Point Cloud Normalization and Canopy Height Model

To prepare the Watershed Segmentation application, first, data set was normalized then Canopy Height Model was generated.



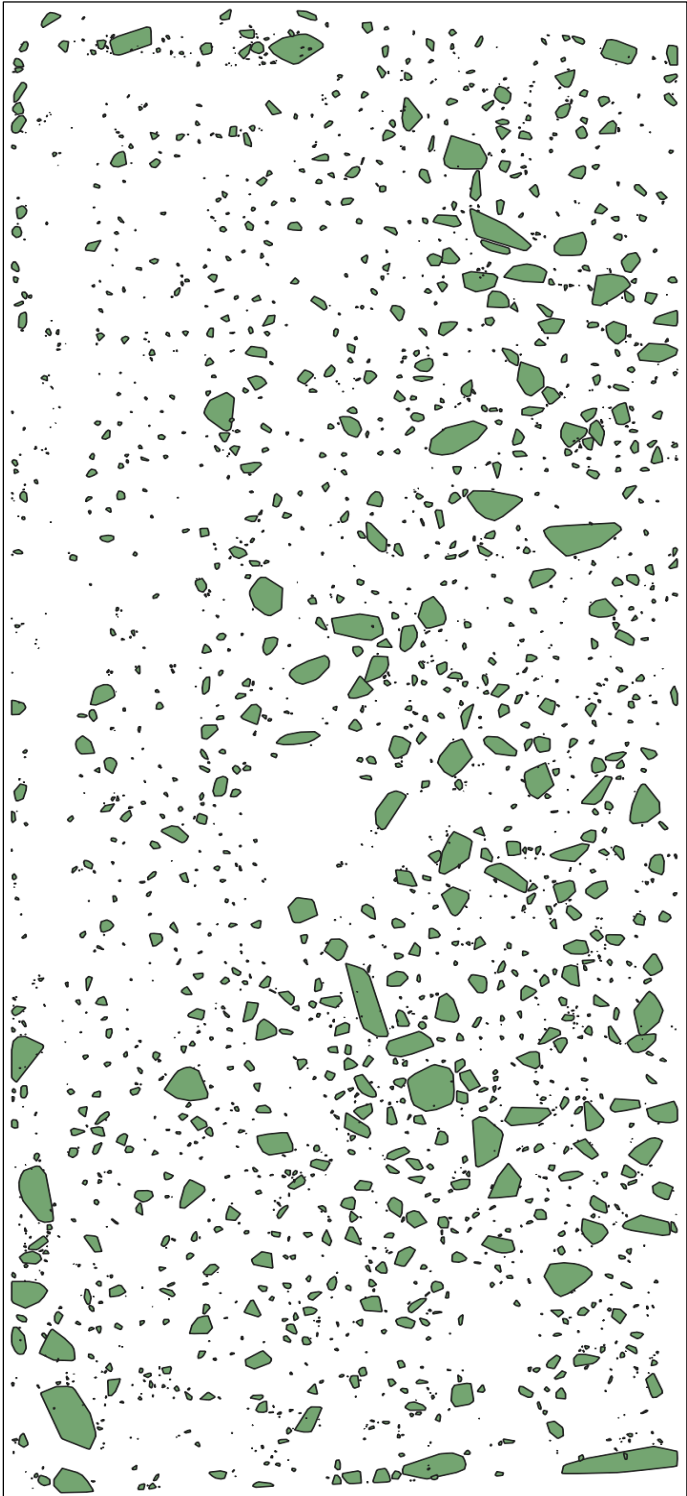
14: Normalized point cloud of Tiny Forest, front isometric view.



15: Canopy Height Model of Tiny Forest, front isometric view.

3.6 Detection and localization of tree crowns

In the Tiny Forest, 2337 trees were detected above 40 cm with the help of Watershed Segmentation Algorithm.

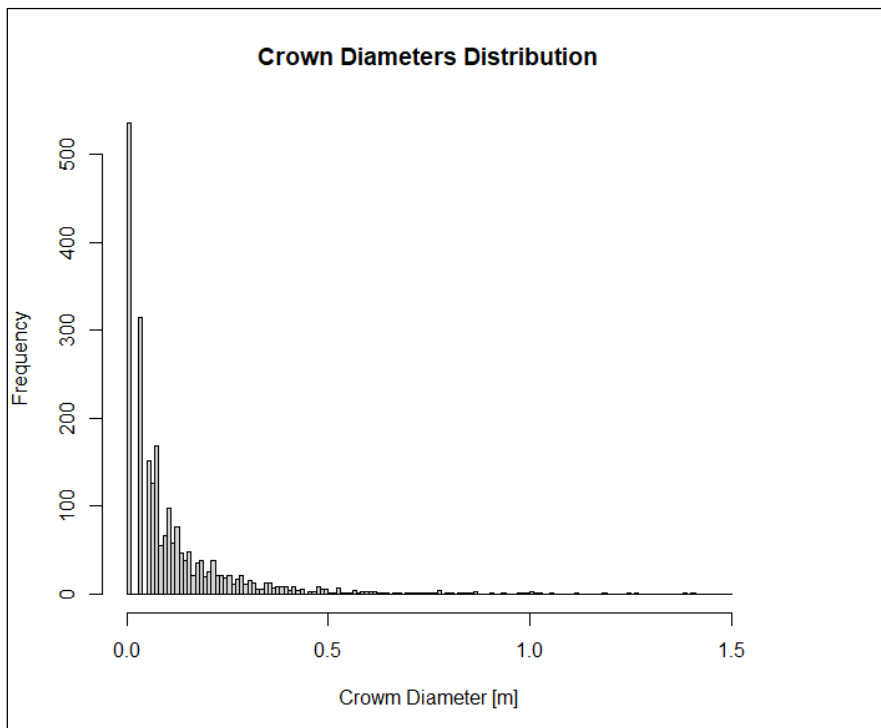


16: Location of the tree crowns in Tiny Forest, top view in QGIS software

3.7 Tree Size Distribution

Inventory of each tree in Tiny Forest was generated with the following formulas and assumptions.

$$\text{CrownRadius} = (\text{CrownArea} / \pi)^{0.5}$$
$$\text{CrownDiameter} = 2 * \text{CrownRadius}$$



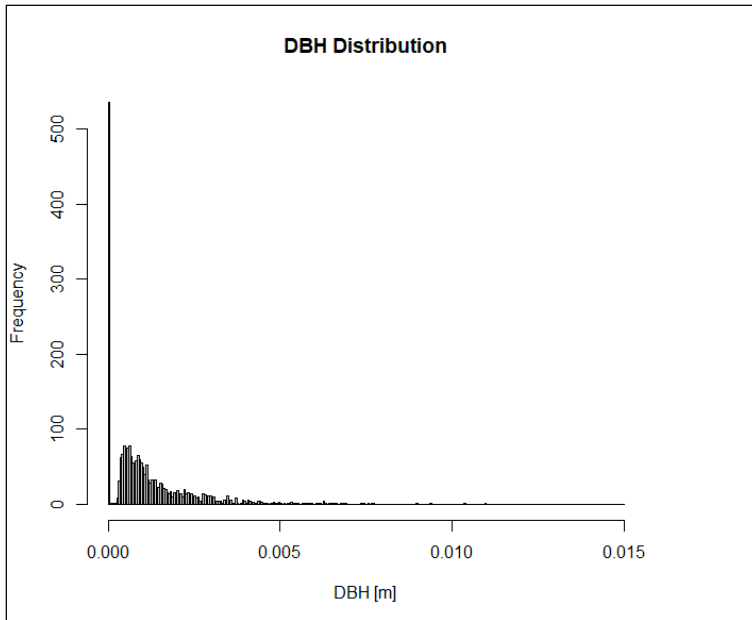
17: Crown Diameters Distribution

Min.	1st Qu.	Median	Mean	3rd Qu.	Max.	
0.00000	0.03568	0.07136	0.12290	0.15139	1.40573	Standard Deviation = 0.165186

2D bounding box (tree height x crown diameter)
 $\text{TreeBoundingBox} = Z(\text{Height}) * \text{CrownDiameter}$

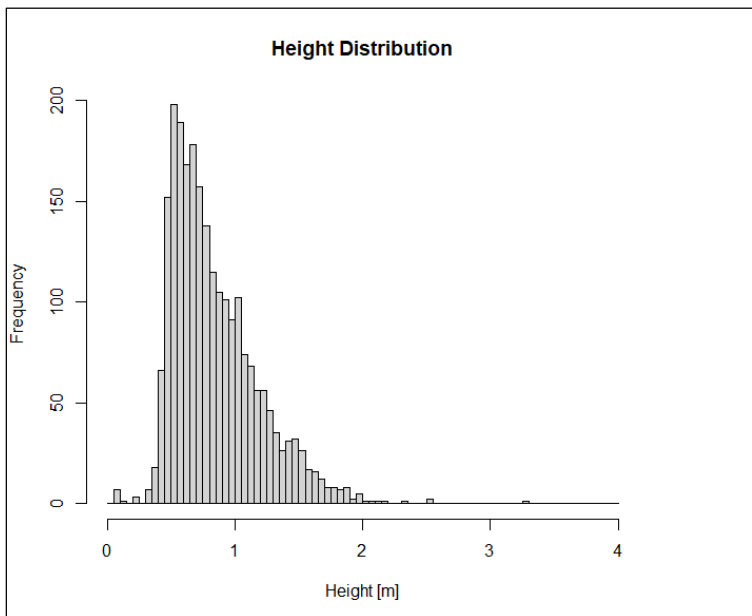
According to Jucker et al. (2016) DBH can be estimated from the tree bounding box (H x CD) with the following power law (parameters for Palearctic temperate mixed forest, table S3). Convert to meter units by division by 100.

$$\text{DBH} = 0.708 * \text{TreeBoundingBox}^{0.753} / 100$$



18: DHB Distribution

Min.	1st Qu.	Median	Mean	3rd Qu.	Max.	
0.000	0.0003547	0.0007940	0.0011374	0.0015045	0.0109674	Standard Deviation = 0.001289792



19: Height Distribution

Min.	1st Qu.	Median	Mean	3rd Qu.	Max.	
0.0525	0.5859	0.7630	0.8417	1.0286	3.2890	Standard Deviation = 0.3378825

$$\text{CrownLength} = 0.6 * Z(\text{Height})$$

$$\text{CrownBaseHeight} = 0.4 * Z(\text{Height})$$

4. CONCLUSION

Even though the heights of the young trees were yet only between 30 and 200 cm, it was possible to detect the correct number of individuals. The tested methods of data processing and segmentation measurements provided information regarding the total biomass, height distribution, DHB distribution and crown diameter distribution. In the future it will be possible, to continuously collect data this way and to precisely show the growth dynamics of Tiny Forests.

To evaluate this still very new and innovative method for urban forests scientifically, it is crucial to gain data right from the beginning. Especially interesting are their growth rate, biomass production & carbon sequestration in comparison to other forests sites. We hope that through new technologies like Slam we will be able to show the effectiveness and potentials of the Miyawaki method as a nature based solution for climate adaption in cities. Moreover, we think that the method can be further developed and that modern technological approaches might help to increase their effectiveness.

Bibliography

- Xu, S., Sun, X., Yun, J., & Wang, H. (2020). A New Clustering-Based Framework to the Stem Estimation and Growth Fitting of Street Trees From Mobile Laser Scanning Data. *IEEE JOURNAL OF SELECTED TOPICS IN APPLIED EARTH OBSERVATIONS AND REMOTE SENSING*, *13*, 3240-3250. doi:10.1109/JSTARS.2020.3001978
- Cabo C, D. P.-G.-A. (2018). Comparing Terrestrial Laser Scanning (TLS) and Wearable Laser Scanning (WLS) for Individual Tree Modeling at Plot Level. *Remote Sensing*, *10*(4), 540. doi:doi.org/10.3390/rs10040540
- Chen, Q. B. (2006). Isolating Individual Trees in a Savanna Woodland Using Small Footprint Lidar Data . *Photogrammetric Engineering & Remote Sensing*, *72*(8), 923–932. doi:10.14358/pers.72.8.923
- Dalponete, M., & Coomes, D. (2016). Tree-centric mapping of forest carbon density from airborne laser scanning and hyperspectral data. *Methods in Ecology and Evolution*, *7*(10), 1236-1245. doi:10.1111/2041-210X.12575
- de Mesnard, L. (2013). Pollution models and inverse distance weighting: Some critical remarks. *Computers & Geosciences*, *52*, 459-469. doi:10.1016/j.cageo.2012.11.002
- di Filippo, A., Javier Sánchez-Aparicio, L., Barba, S., Antonio Martín-Jiménez, J., Mora, R., & González Aguilera, D. (2018). Use of a Wearable Mobile Laser System in Seamless Indoor 3D Mapping of a Complex Historical Site. *Remote Sensing*, *10*(1987). doi:10.3390/rs10121897
- Dubayah, R. B. (2020). The Global Ecosystem Dynamics Investigation: High-resolution laser ranging of the Earth's forests and topography. *Science of Remote Sensing*, <https://doi.org/10.1016/j.srs.2020.100002>.
- Duncanson, L., Cook, B., Hurtt, G., & Dubayah, R. (2014). An efficient, multi-layered crown delineation algorithm for mapping individual tree structure across multiple ecosystems. *Remote Sensing of Environment*, *154*, 378-386. doi:10.1016/j.rse.2013.07.044
- Gargoum, S., & El-Basyouny, K. (2019). Effects of LiDAR Point Density on Extraction of Traffic Signs: A Sensitivity Study. *Transportation Research Record: Journal of The Transportation Research Board*, *2673*(1), 41-51. doi:10.1177/0361198118822295
- Gollob, C., Ritter, T., & Nothdurft, A. (2020). Comparison of 3D Point Clouds Obtained by Terrestrial Laser Scanning and. *Data*, DOI: 10.3390/data5040103.
- Hämmerle, M., & Höfle, B. (2014). Effects of Reduced Terrestrial LiDAR Point Density on High-Resolution Grain Crop Surface Models in Precision Agriculture. *Agriculture and Forestry: Sensors, Technologies and Procedures*, *14*(12), 24212-24230. doi:10.3390/s141224212
- Ke, Y., & Quackenbush, L. J. (2011). A review of methods for automatic individual tree-crown detection and delineation from passive remote sensing. *International Journal of Remote Sensing*, *32*(17), 4725–4747. doi:10.1080/01431161.2010.494184
- Li, W., Guo, Q., Jakubowski, M., & Kelly, M. (2012). A New Method for Segmenting Individual Trees from the Lidar Point Cloud. *PHOTOGRAMMETRIC ENGINEERING & REMOTE SENSING*, *78*(1), 75-84. doi:10.14358/PERS.78.1.75
- Lindberg, E., & Holmgren, J. (2017). Individual Tree Crown Methods for 3D Data from Remote Sensing. *Current Forestry Reports*, *3*. doi:10.1007/s40725-017-0051-6
- Liu, J., Skidmore, A., Heurich, M., & Wang, T. (2017). Significant effect of topographic normalization of airborne LiDAR data on the retrieval of plant area index profile in mountainous forests. *ISPRS Journal of Photogrammetry and Remote Sensing*/ISPRS Journal of Photogrammetry and Remote Sensing, *132*, 77-87. doi:10.1016/j.isprsjprs.2017.08.005

- Maguya, A., Junttila, V., & Kauranne, T. (2013). Adaptive algorithm for large scale dtm interpolation from lidar data for forestry applications in steep forested terrain. *ISPRS Journal of Photogrammetry and Remote Sensing*, 85, 74-83. doi:10.1016/j.isprsjprs.2013.08.005
- Nocerino, E., Menna, F., Remondino, F., Toschi, I., & Rodríguez-González, P. (2017). Investigation of indoor and outdoor performance of two portable mobile mapping systems. In F. Remondino, & M. Shortis (Hrsg.), *Videometrics, Range Imaging, and Applications XIV*. 10332. SPIE. doi:10.1117/12.2270761
- Pirotti, F., & Tarolli, P. (2010). Suitability of LiDAR point density and derived landform curvature maps for channel network extraction. *HYDROLOGICAL PROCESSES*, 24, 1187–1197. doi:10.1002/hyp.7582
- Soille, P. (2004). *Morphological Image Analysis*. doi:10.1007/978-3-662-05088-0 (2 Ausg.). Springer-Verlag Berlin Heidelberg 2003 and 2004. doi:10.1007/978-3-662-05088-0
- Solutions: ZEB Horizon*. (15. February 2021). Von GeoSLAM: <https://geoslam.com/solutions/zeb-horizon/> abgerufen
- Wulder, M., Niemann, K., & Goodenough, D. (2000). Local Maximum Filtering for the Extraction of Tree Locations and Basal Area from High Spatial Resolution Imagery. *REMOTE SENSING OF ENVIRONMENT*, 73(1), 103–114. doi:10.1016/S0034-4257(00)00101-2
- Zhang, K., Chen, S.-C., Whitman, D., Shyu, M.-L., Yan, J., & Zhang, C. (2003). A Progressive Morphological Filter for Removing Nonground Measurements From Airborne LIDAR Data. *IEEE TRANSACTIONS ON GEOSCIENCE AND REMOTE SENSING*, 41, 872 - 882. doi:10.1109/TGRS.2003.810682
- Zhang, W., Qi, J., Wan, P., Wang, H., Xie, D., Wang, X., & Yan, G. (2016). An Easy-to-Use Airborne LiDAR Data Filtering Method Based on Cloth Simulation. *Airborne Laser Scanning*, 8(6), 501. doi:10.3390/rs8060501